horticulturae

MDPI

Article

Biodegradability of Innovative Bio-Based Films Enriched with Monoammonium Phosphate

Sara Paliaga [1], Luigi Badalucco [1], Delia Francesca Chillura Martino [2], Veronica Concetta Ciaramitaro [2], Silvia Rita Stazi [3], Enrica Allevato [4], Vittorio Vinciguerra [5] and Vito Armando Laudicina [1,6,*]

[1] Department of Agricultural, Food and Forest Sciences, University of Palermo, 90128 Palermo, Italy; sara.paliaga@unipa.it (S.P.); luigi.badalucco@unipa.it (L.B.)
[2] Department of Biological, Chemical and Pharmaceutical Sciences and Technologies, University of Palermo, 90128 Palermo, Italy; delia.chilluramartino@unipa.it (D.F.C.M.); veronicaconcetta.ciaramitaro@unipa.it (V.C.C.)
[3] Department of Chemical, Pharmaceutical and Agricultural Sciences, University of Ferrara, 44121 Ferrara, Italy; silviarita.stazi@unife.it
[4] Department of Environmental and Prevention Sciences, University of Ferrara, 44121 Ferrara, Italy; enrica.allevato@unife.it
[5] Department for Innovation in Biological, Agro-Food and Forest Systems, University of Tuscia, 01100 Viterbo, Italy; vincigue@unitus.it
[6] NBFC, National Biodiversity Future Center, 90133 Palermo, Italy
* Correspondence: vitoarmando.laudicina@unipa.it

Abstract

The widespread use of conventional plastic mulch films in agriculture contributes significantly to soil pollution due to their non-biodegradable nature. This study explores the potential of novel bio-based mulch films composed of chitosan, carboxymethyl cellulose, and sodium alginate, formulated in different ratios (1:1 and 17:3), with or without enrichment with monoammonium phosphate (MAP), to serve as biodegradable films with potential nutrient-releasing functionality as alternatives to conventional plastics. A multi-analytical approach, including elemental and isotopic analysis (EA-IRMS), biodegradation assays, and pyrolysis–gas chromatography–mass spectrometry (Py-GC-MS), was employed to assess their chemical properties, degradation behavior, and environmental compatibility. The results demonstrated that the 1:1 films, both with and without MAP, achieved over 90% biodegradation within 120 days under controlled soil conditions, in agreement with international criteria for soil biodegradability. In contrast, the 17:3 films showed reduced degradation, especially without MAP enrichment, highlighting the influence of polymer composition on microbial degradation. Isotopic tracing confirmed MAP integration and revealed composition-dependent fractionation effects. Py-GC-MS provided structural fingerprints of film components and putatively annotated nitrogen-containing compounds indicative of chitosan presence. Overall, these results demonstrate that the 1:1 films can be considered viable, multifunctional, and soil-friendly alternatives to conventional plastic mulches for sustainable agriculture.

Keywords: bio-based mulching films; biopolymers; soil biodegradation; nutrient-enriched films; sustainable agriculture; GC-pyrolisis

Check for updates

Academic Editors: Wilfried Rozhon and Maria Roulia

Received: 26 December 2025
Revised: 16 February 2026
Accepted: 17 February 2026
Published: 21 February 2026

Copyright: © 2026 by the authors. Licensee MDPI, Basel, Switzerland. This article is an open access article distributed under the terms and conditions of the Creative Commons Attribution (CC BY) license.

1. Introduction

The global consumption of plastics in agriculture reaches approximately 16 million tons annually, with plastic films for soil mulching accounting for over 10% [1]. The widespread

use of these films significantly contributes to better agricultural outcomes, such as higher crop yields, faster harvesting, reduced need for herbicides and pesticides, more stable soil temperature, and optimized water and fertilizer conservation [2]. These benefits have made plastic films an essential tool in modern farming practices, leading to increased demand while aggravating issues related to plastic waste generation and soil contamination. Most plastic films used in agriculture, including polyethylene, polyvinyl chloride, and polybutylene-based plastics, are non-biodegradable, leading to their accumulation in the environment of plastic waste, which is often abandoned in the field or burned, releasing harmful pollutants into the air and soil [3]. Mulch films alone contribute to an estimated 39% of soil contamination [4], with plastic residues reaching up to 200 kg ha^{-1}, negatively affecting soil quality, crop development, and overall yield [5,6]. In this context, biodegradable mulching films emerge as a promising alternative to conventional plastic films, as they can be incorporated into the soil at the end of the growing season, naturally degrading through microbial activity and providing an environmentally friendly solution. The spread of biodegradable mulching films offers significant economic and environmental advantages. Several types of biodegradable films, such as those combining starch materials often marketed as biodegradable, including polyvinyl alcohol, or partially biodegradable materials like starch with polyethylene-co-acrylic acid, had an uncertain outcome in research and development [7,8]. One particularly promising option is poly(ε-caprolactone) (PCL), a fully biodegradable polymer derived from non-renewable resources like crude oil [9]. When combined with starch, PCL can create a cost-effective and environmentally friendly material suitable for agricultural mulching [2]. Although PCL is often considered a sustainable alternative to conventional plastics, its environmental impact remains significant. PCL is derived from petroleum-based raw materials, which means its production is inherently linked to the extraction and refining of fossil fuels. These processes are energy-intensive and contribute to the exhaustion of non-renewable resources. In addition, while PCL is biodegradable under certain conditions, the process is slow in difficult environmental conditions such as in soil. As a result, it can persist for years, contributing to microplastic pollution and posing a threat to soil health. Therefore, the scientific community is shifting its focus to bio-based biodegradable polymers, i.e., derived from renewable sources—such as plants, algae, and agricultural residues—which are gaining attention for their potential to reduce reliance on fossil resources and lower greenhouse gas (GHG) emissions. Life cycle assessments indicate that bio-based plastics can significantly decrease environmental impact, with some studies reporting a 40–50% reduction in fossil fuel consumption and a 45–55% decrease in GHG emissions for polyethylene furanoate (PEF) production compared to polyethylene terephthalate (PET) [10,11]. Despite their advantages, bio-based plastics currently represent only 1.5% of the total plastics market, accounting for approximately 5.9 million tons, although important gains are expected in the coming years [12].

While bio-based plastics offer a promising alternative to petroleum-based plastics, their environmental benefits depend not only on their origin but also on their ability to degrade effectively in the soil. A bio-based material does not necessarily mean it is biodegradable under agricultural conditions. Some bio-based polymers, such as bio-polyethylene (bio-PE) or bio-polypropylene (bio-PP), show similar degradation properties to their fossil-based counterparts, maintaining long-term persistence in the environment [13]. Therefore, evaluating the biodegradability rate of agricultural films is essential to ensure they do not contribute to plastic accumulation in the soil. The biodegradability of plastic films can be assessed through various standardized testing methods that measure both the extent and rate of their breakdown into carbon dioxide, water, and biomass through microbial activity.

Currently, there are several internationally recognized standard methods for assessing the biodegradability of plastics in soil, such as ISO 17556:2019 [14] and EN 17033:2018 [15].

These methods primarily evaluate the O_2 consumption or the release of CO_2 over time under controlled conditions, typically at soil temperatures between 20 °C and 28 °C. More specifically, biodegradation is expressed as a percentage value given by the ratio between the evolved CO_2-C and the total C content of the tested material. To confirm the biodegradability of a material, these standards require that at least 90% of the carbon of the tested material be converted into CO_2 within two years, both in absolute terms and relative to a reference material such as microcrystalline cellulose.

Biodegradation under aerobic conditions can be described using the following general equation [16,17]:

$$C_{plastic} + O_2 \rightarrow CO_2 + H_2O + C_{residue} + C_{biomass} \quad (1)$$

The biodegradation process evolves in three key stages. First, large polymer chains are broken down by extracellular microbial enzymes into smaller, soluble units. This depolymerization, often the rate-limiting step, facilitates microbial access. Second, these smaller fragments are absorbed and incorporated within microbial cells, which, after, mineralize them into CO_2 and H_2O [17,18] by accelerated microbial activity, further enzyme secretion, and changes in smaller fragment properties. Finally, a plateau phase occurs as easily degradable fractions are exhausted or nutrients become limited, slowing degradation. The duration of each phase varies with polymer type, conditions, and microbial communities, and understanding them is key to optimizing biodegradability.

Assessing the biodegradability of agricultural films is essential to prevent their accumulation in soils and to mitigate the long-term environmental impact of plastic residues. A comprehensive understanding of their ecological fate requires a detailed characterization of their elemental and isotopic composition, which provides well-defined insights into their intrinsic properties, degradation mechanisms, and interactions within the soil matrix [19]. Among the analytical techniques available, gas chromatography coupled with pyrolysis (GC-pyrolysis) is a powerful tool for investigating the structural composition of biodegradable plastics [20]. This approach allows the annotation of degradation products, the monitoring of polymer stability over time, and the elucidation of degradation pathways under different environmental conditions [21].

In light of the rising environmental concerns surrounding traditional plastic films in agriculture, the potential of innovative bio-based films as a sustainable alternative is explored. Specifically, this study aims to evaluate the biodegradability of novel films composed of chitosan, carboxymethyl cellulose, and sodium alginate, formulated in varying mass ratios and supplemented with or without monoammonium phosphate as a nutrient source, under controlled soil temperature and moisture conditions. Furthermore, the elemental and isotopic composition of these films will be characterized to elucidate their intrinsic properties and potential environmental fate. Finally, pyrolysis–gas chromatography–mass spectrometry (Py-GC-MS) analysis will be employed to further clarify the structural characteristics of these bio-based films. Through this comprehensive investigation, a thorough assessment of the reliability and environmental impact of these innovative bio-based films is expected, thereby contributing to the development of sustainable agricultural practices.

2. Materials and Methods

2.1. Bio-Based Films Preparation

The biodegradable mulch films were produced in the laboratory by using the solvent casting technique described in [22]. Briefly, two dispersions were prepared: the first was obtained by dissolving carboxymethyl cellulose (CMC; Mw 75–150 kDa,

CAS 9005-38-3), a water-soluble cellulose derivative, in distilled water. The second was obtained by dissolving chitosan (CS; Mw 150–700 kDa, degree of acetylation > 75%, CAS 9012-76-4), sodium alginate (SA; average Mw ~250 kDa, degree of substitution 0.9, CAS 9004-32-4), and glycerol in 2.0% (*v*/*v*) aqueous acetic acid solution (CS/SA). All the reagents used for producing the films were purchased from Merck Life Sciences S.r.l. (Milan, Italy). To obtain the films, the two dispersions CS/SA and CMC were mixed in two different mass ratios, 1:1 or 17:3, respectively. Once homogenized, the dispersions were immediately spread within a plastic Petri dish and left at room temperature for drying. From now on, the films will be referred to as 1:1 or 17:3, depending on the mass ratio of the dispersions used. Generally, after 24 h (the drying period slightly varied depending on air temperature and humidity), the films were manually peeled off the Petri dishes. The resulting films showed an average thickness of 150 ± 20 µm. Further bio-based mulch films enriched with monoammonium phosphate ($NH_4H_2PO_4$—MAP) were prepared as described above, by adding 30, 70, or 90 wt% of MAP (calculated with respect to the average dry weight of the polymer film) to the CMC dispersion. More details about preparation, mechanical properties, and water interaction of the films are reported in [22,23].

2.2. Films' Elemental and Isotopic Analysis

An elemental analyzer–isotope ratio mass spectrometer (EA-IRMS, Elementar Vario Micro Cube—coupled to Isoprime 100) system was used to determine C and N contents of these films and their isotopic signatures (i.e., $\delta^{13}C$ and $\delta^{15}N$). Film samples (1:1 and 17:3 ratios), either without MAP or with 30%, 70%, and 90% MAP added, were dried for 12 h at 30 °C. About 3 mg of bio-based mulch films and 1 mg of commercial Mater-Bi (Novamont) and polyethylene (PE) reference films were weighed. Every sample was analyzed in triplicate. The isotopic standards used for the analysis were sulfanilamide ($\delta^{13}C = -27.3$ ‰; $\delta^{15}N = -1.0$ ‰), Carrara Marble by IGG-CNR of Pisa ($\delta^{13}C = 2.1$ ‰; $\delta^{15}N$ = n.d.), and IAEA-Caffeine ($\delta^{13}C = -27.8$ ‰; $\delta^{15}N = 1.0$ ‰).

Total P content in the films was determined after mineralization using the Spectroquant® Phosphate test with a spectrophotometer (UVmini-1240, Shimadzu Italia srl, Milan, Italy), monitoring the formation of a yellow-orange complex. The wet digestion was conducted as follows: 0.5 g of film was weighed into a porcelain crucible and placed in a cold muffle furnace. The temperature was set to reach 500 °C over approximately 3 h, and the samples were left to rest overnight. The day after, the cooled samples were added with 5 mL of HNO_3 and 5 mL of 30% H_2O_2. The samples were then placed on a heating plate at 250 °C for 2 h. After cooling, the digested samples were recovered using 2% HNO_3 [24].

2.3. Films' Biodegradability Test

The soil used for the films' biodegradability test was collected from the topsoil (0–20 cm depth) of a citrus orchard at the Department of Agricultural, Food, and Forestry Sciences, University of Palermo, Italy (38°10′66.6″ N, 13°35′03.9″ E). After the sampling, the soil was air-dried, sieved at <2 mm, and amended with 1.5% (*w*/*w*) mature cow manure. The main soil characteristics were loamy-sand texture, pH and EC (1:2.5, *w*/*v*, in water) of 7.1 and 0.6 dS m^{-1}, respectively, total organic C (TOC) of 49 g kg^{-1}, total nitrogen (TN) of 3.9 g kg^{-1}, available P of 68.5 mg kg^{-1}, and cation exchange capacity (CEC) of 32.7 $cmol^+$ kg^{-1}. Before starting the experiment, the soil was moistened up to approximately 50% of its water holding capacity (corresponding to ~12% gravimetric water content) and then pre-incubated at 20–22 °C in the dark for 14 days, to restore the soil microbial community.

Next, the different films, 1:1 or 17:3 with or without 90% MAP-enrichment, cut into pieces less than 5 mm in size, were added to the soil at a ratio of 1.5% weight basis, corresponding to 0.75 g of film per 50 g of dry soil.

The soils with films were incubated in 250 mL glass jars, sealed with rubber stoppers containing silicone septa, and placed in the dark at 25 ± 3 °C to monitor the CO_2 production rate during a 120-day incubation. The experimental setup and calculation of biodegradation rate were based on the principles in [14], with adaptations to soil type, incubation system, and sampling frequency. For each treatment, four replicates were performed. In parallel, four further soil sub-aliquots, without film addition, were similarly incubated as controls (CTR, basal respiration). The CO_2 accumulated during incubation in the headspace of the glass jars was determined at intervals by injecting 1 mL of air from each jar into a gas chromatograph (TraceGC, Thermo Fisher Scientific, Milan, Italy) equipped with a thermal conductivity detector and a Poropak Q column, using He as the carrier (oven 50 °C, injector at 225 °C, column flow 40 mL/min, split mode 10:1).

The percentage of biodegradation was calculated as the ratio between the cumulative net CO_2–C evolved from film-amended soils and the theoretical maximum CO_2–C expected from complete mineralization of the carbon contained in each film, according to ISO 17556, as expressed in Equation (2):

$$\text{Biodegradation } (\%) = \frac{CO_2\text{–}C_{net}}{CO_2\text{–}C_{theoretical}} \times 100 \quad (2)$$

where CO_2–C_{net} is the cumulative CO_2–C evolved from film-amended soil after subtraction of the control respiration, and CO_2–$C_{theoretical}$ is the amount of CO_2–C expected from complete oxidation of the carbon initially added with each film, calculated from its measured carbon content (%C) and the applied film mass.

2.4. Film Analysis by Pyrolysis–Gas Chromatography–Mass Spectrometry

Moreover, the films 1:1, with and without MAP enrichment, and the individual pure components (CMC, SA, and CS) and a commercial Mater-Bi sample were analyzed by pyrolysis–gas chromatography–mass spectrometry (Py-GC-MS) in order to characterize their chemical structure according to the different components. Based on the results of the soil biodegradability tests (Section 3.2), only the 1:1 film formulations were selected for further detailed chemical characterization by Py-GC-MS. The 17:3 films did not reach the threshold for soil biodegradability under the tested conditions and were therefore excluded from subsequent analyses. The commercial Mater-Bi film was analyzed as a benchmark material, as it represents a widely used biodegradable mulch film composed of a starch fraction combined with fossil-based PBAT, thus providing a useful comparison with the fully bio-based films developed in this study. Pieces of 1.5–2.0 mg of film samples, reduced to powder, and of individual pure components were introduced by a special syringe into a vertical furnace pyrolyzer Pyrojector II (SGE, Victoria, Australia) pre-heated at 450 °C, under helium carrier gas at a pressure of 100 kPa, coupled to a gas chromatograph-mass spectrometer system GCMS-QP5050A (Shimadzu, Kyoto, Japan) equipped with a Restek Rtx®-5MS (30 m × 0.25 mm i.d.) capillary column (Restek, Bellefonte, PA, USA). Helium was the carrier gas in the injector (280 °C, split 1:20) at a pressure of 70 kPa. The oven program was: 45 °C isotherm for 2 min, 10 °C min^{-1} up to 300 °C, held for 40 min. The mass spectrometry interface was kept at 280 °C, and the ion source operated at 180 °C in electron impact mode at 70 eV. Mass spectra were acquired in full scan mode from 40 to 400 m/z. Pyrolysis products were putatively annotated by interpretation of mass spectra, by comparison with the NIST computer library and literature data [25–27].

2.5. Statistical Analysis

Elemental and isotopic data, obtained from triplicate analytical measurements, are reported as mean ± standard error (SE) and were primarily used for descriptive and comparative purposes. Cumulative CO_2–C production from film-amended soils was corrected for basal soil respiration by subtracting the mean CO_2–C evolved from control soils incubated without films. Biodegradation percentages were calculated from these net CO_2–C values as described in Equation (2).

Statistical analyses were performed on the resulting biodegradation percentages, which represent treatment-level responses corrected for control respiration. Differences among film formulations were evaluated by one-way analysis of variance (ANOVA), followed by Tukey's honestly significant difference (HSD) post hoc test. Statistical significance was accepted at $p < 0.05$. Biodegradation and CO_2–C production data are reported as mean ± standard deviation (SD) of four independent replicates ($n = 4$). Statistical analyses were performed using SPSS 2021.

3. Results and Discussion

3.1. Elemental Composition and Isotopic Signatures of

The elemental and isotopic analyses, reported in Table 1 and Figure 1, show the impact of polymer composition and MAP addition on the chemical characteristics of films. The results clearly show that the increase in MAP content leads to a progressive decrease in carbon (%C) and an increase in nitrogen (%N) and phosphorus (%P), which are consistent with the inorganic nature of MAP.

Table 1. Carbon (C), nitrogen (N), and phosphorus (P) content (weight %) and C/N ratio of different films. Values represent mean ($n = 3$) ± standard error (SE). n.d., not detectable.

Film Type	C (wt%)		$\delta^{13}C$ (‰)		N (wt%)		$\delta^{15}N$ (‰)		C/N Ratio	P (wt%)	
	Mean	±SE	Mean	±SE	Mean	±SE	Mean	±SE		Mean	±SE
Mater-Bi	45.04	2.70	−24.6	0.0	n.d.		n.d.		n.d.	n.d.	
PET	69.70	4.27	−27.3	0.0	n.d.		n.d.		n.d.	n.d.	
1:1 + MAP 0%	33.70	0.96	−26.6	0.1	1.49	0.07	−4.7	0.1	22.60	n.d.	
1:1 + MAP 30%	22.37	0.98	−26.9	0.1	2.79	0.20	8.0	0.4	8.03	4.31	0.46
1:1 + MAP 70%	17.85	0.77	−26.9	0.1	4.68	0.26	6.5	0.1	3.81	9.06	0.96
1:1 + MAP 90%	15.84	0.60	−26.8	0.1	5.59	0.37	5.8	0.1	2.83	12.80	1.20
17:3 + MAP 0%	34.09	1.86	−25.7	0.2	2.24	0.09	−4.3	0.1	15.22	n.d.	
17:3 + MAP 30%	26.67	1.52	−25.5	0.2	2.61	0.23	4.6	0.2	10.22	3.41	0.64
17:3 + MAP 70%	20.92	1.03	−25.4	0.2	4.05	0.30	5.7	0.3	5.16	8.06	0.93
17:3 + MAP 90%	19.98	0.91	−25.2	0.2	5.99	0.12	4.7	0.2	3.34	10.11	1.97

The %C in the 1:1 films decreased significantly with increasing MAP content, reflecting the dilution of the organic matrix by a C-free salt. The isotopic signature of carbon ($\delta^{13}C$) shows a moderate shift from –26.6‰ to –26.9‰ with the addition of MAP. These variations are relatively small (≤0.3‰) and, although within the analytical precision (±0.1‰), are more plausibly attributed to compositional heterogeneity within the films rather than to true isotopic fractionation involving carbon. In particular, previous XRD analyses performed by the authors on the same polysaccharide-based films demonstrated the presence of chitosan-rich domains and composition-dependent structural heterogeneity, which may result in local variations in the relative contribution of the different biopolymers to the bulk carbon isotopic signal [22]. The nitrogen content (%N) in the 1:1 films shows a clear increase with MAP addition, consistent with the introduction of NH_4^+ from MAP. The N isotopic signature ($\delta^{15}N$) further confirms the effective incorporation of MAP. While the MAP-free film shows a negative $\delta^{15}N$, typical of chitosan, the addition of 30% MAP results

in a sharp enrichment (+8‰), reflecting the high ^{15}N content typical of industrial MAP, that often exhibits positive $\delta^{15}N$ values. Indeed, it can vary from +2‰ to +10‰ or even more, depending on the synthesis [28]. This indicates that the MAP is effectively incorporated into the matrix and strongly influences its isotopic signature. However, with 70% and 90% MAP addition, $\delta^{15}N$ values unexpectedly decrease to 6.5‰ and 5.8‰, respectively. This behavior suggests the onset of a non-homogeneous nitrogen distribution within the polymer matrix at high MAP loadings. In this context, localized MAP-rich regions and polymer-rich domains may coexist, leading to non-ideal isotopic mixing between chitosan-derived nitrogen and ammonium-derived nitrogen (see conceptual model in Supplementary Figure S1). As a result, the contribution of MAP-derived nitrogen to the bulk $\delta^{15}N$ signal may become non-proportional at high salt loadings, indicating a practical limit to homogeneous MAP incorporation within the polymeric network.

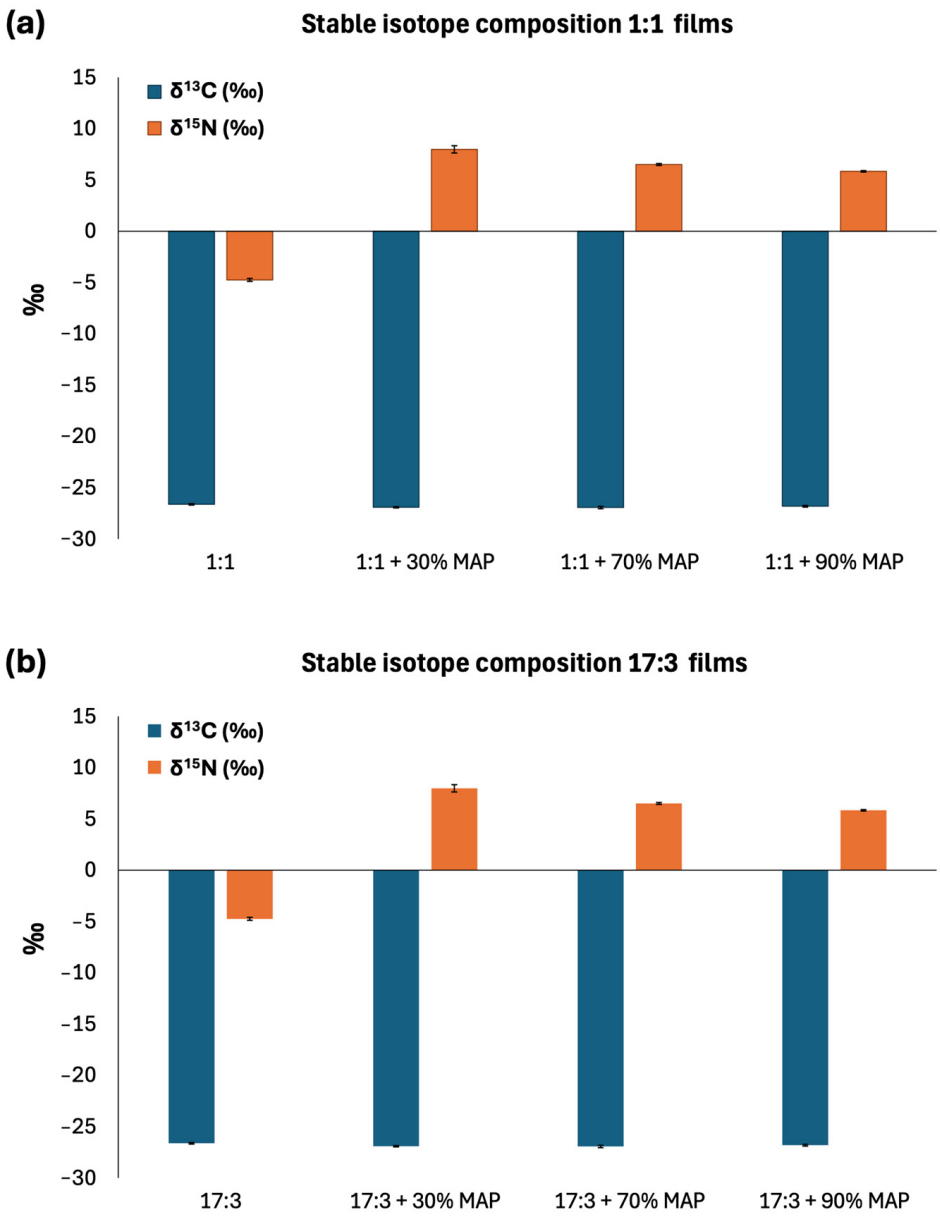


Figure 1. Stable isotopic composition ($\delta^{13}C$ and $\delta^{15}N$) of films 1:1 (**a**) and 17:3 (**b**). The blue bars represent $\delta^{13}C$ (‰), while the orange bars indicate $\delta^{15}N$ (‰). Values are reported as means (n = 3) ± standard error (SE).

In the 17:3 films (with higher chitosan content), the %C also decreases up to 41% with MAP addition, but the drop is less pronounced than in the 1:1 films. This is likely because the 17:3 film has a higher chitosan content and, therefore, more C bound to N. Interestingly, while $\delta^{13}C$ in 1:1 films became more negative with MAP addition, in 17:3 films, it shifts slightly toward more positive values (from –25.7‰ to –25.2‰). This inverse trend may reflect different interaction dynamics between MAP and the more abundant amine groups in chitosan, which could influence the relative contribution of chitosan-rich domains to the bulk carbon isotopic signal, rather than indicating true carbon isotopic fractionation.

Similarly, %N in 17:3 films increased markedly with MAP (up to +167%), confirming the incorporation of the N-rich salt. $\delta^{15}N$ also showed a consistent enrichment up to 70% MAP, followed by a decrease at 90% MAP (to +4.7‰), again indicating the onset of non-ideal nitrogen distribution and saturation effects at high MAP loadings, in line with the behavior observed for the 1:1 films.

No significant difference in %P was observed between the 1:1 and 17:3 films at equivalent MAP contents. This suggests that P incorporation is not substantially affected by the ratio of chitosan to carboxymethyl cellulose in the polymer blend. Similar %P values suggest that bulk phosphorus content mainly reflects the amount of MAP introduced during film preparation, with limited influence of polymer composition on total P content. This linear increase in %P, together with the absence of matrix-specific variations, supports the hypothesis that phosphate is retained mainly through physical incorporation or electrostatic interactions (e.g., with protonated amines in chitosan or hydroxyls in carboxymethyl cellulose), rather than through covalent bonds.

The negative $\delta^{13}C$ values across all samples confirm the use of organic polymers as the carbon source. Differences in $\delta^{13}C$ between the 1:1 and 17:3 films may reflect variability in the carbon source material, consistent with previous findings by Perini et al. [29], who reported $\delta^{13}C$ values of –21.7‰ for crustacean-derived chitosan and –13.8‰ for fungal chitosan. The $\delta^{15}N$ value of –4.7‰ in MAP-free films aligns with the fungal origin, as suggested by Perini et al. (–4.2‰ for fungal vs. –2.3‰ for crustacean chitosan). Overall, the addition of MAP significantly alters both the elemental composition and isotopic signatures of the films. In particular, $\delta^{15}N$ proves to be a reliable tracer of MAP-derived nitrogen incorporation, while the combined elemental and isotopic trends highlight the influence of film structure and polymer distribution on the resulting bulk isotopic signals.

As expected, when compared to the commercial films—polyethylene (PE) and Mater-Bi—the innovative developed bio-based films show distinctive and advantageous characteristics. Both PE and Mater-Bi displayed high carbon content (69.7% and 45.0%, respectively) and lacked detectable N and P, confirming their inert and nutrient-deficient nature.

3.2. Films' Biodegradation

As expected, the CTR exhibited the lowest cumulative CO_2-C evolution throughout the incubation, reflecting the baseline microbial activity of the soil (Figure 2). Conversely, all film-amended samples showed significantly higher cumulative CO_2-C production than the CTR, resulting in different biodegradation percentages over time among film-amended samples (Figure 2).

The initial phase (0–30 days) was characterized by a rapid surge in CO_2-C across all film treatments, suggesting a prompt microbial breakdown of the more labile film components. This initial surge in CO_2–C release corresponds to the steep increase in biodegradation percentages observed during the same incubation period (Figure 3). The absence of a distinct lag phase indicates an immediate microbial response, which may reflect both the rapid utilization of easily accessible carbon fractions within the films and a stimulation of soil microbial activity following film addition. This behavior is consistent

with previous studies reporting fast mineralization of readily available carbon sources in bioplastics under soil conditions [25]. Subsequently, the rate of CO_2-C evolution decreased, indicating a shift towards the degradation of more recalcitrant film fractions or the formation of degradation byproducts that are less readily metabolized. Consistent with their higher cumulative CO_2–C production (Figure 2), 1:1 and 1:1 + MAP films reached biodegradation levels exceeding 90% within 100 days (Figure 3). This indicates a rapid and efficient biodegradation of these materials, likely related to their balanced polymer composition and to the higher proportion of hydrophilic polysaccharide domains (e.g., carboxymethyl cellulose and sodium alginate), which can enhance water uptake and microbial accessibility. Interestingly, the 1:1 film, characterized by a balanced composition of carboxymethyl cellulose, sodium alginate, and chitosan, demonstrated slightly higher biodegradability compared to the 17:3 film, particularly during the initial phase. This discrepancy could be attributed to the higher carboxymethyl cellulose content in the 1:1 film, a polymer known for its susceptibility to microbial degradation [30]. In contrast, the 17:3 film, characterized by a higher chitosan/sodium alginate content relative to carboxymethyl cellulose, may exhibit a more heterogeneous and compact polymer organization, potentially limiting microbial access and enzymatic degradation. The addition of monoammonium phosphate (MAP) significantly enhanced the biodegradability of both film types, especially the 17:3 film. The enhanced CO_2–C evolution observed during the early stages of incubation in MAP-amended treatments suggests that nutrient availability stimulated microbial activity and accelerated the mineralization of film-derived C. Given that N and P are key elements controlling microbial growth and enzyme production, MAP addition likely promoted biodegradation through a general nutrient stimulation mechanism rather than a polymer-specific chemical effect [31]. MAP likely acted as a readily available nutrient source, stimulating microbial growth and metabolic activity, thereby accelerating film decomposition. The pronounced effect of MAP on the 17:3 film suggests that its structure or composition may limit microbial activity under nutrient-limited conditions. The observed plateauing of CO_2-C production and the gradual leveling off of biodegradation percentages in the later stages of the experiment suggest a progressive depletion of readily degradable substrates or the accumulation of more resistant degradation products. This trend is consistent with previous research on the biodegradation kinetics of biopolymers, where a biphasic degradation pattern is often observed, characterized by an initial rapid phase followed by a slower, more prolonged phase [32]. However, after 95 days, biodegradation of all the films tested had reached a clear plateau (Figure 3), with the exception of the 1:1 film, which continued to degrade slowly, reaching 96% biodegradation at the end of the 120-day incubation period.

In conclusion, this study demonstrates that 1:1 films, whether enriched with MAP or not, can be considered biodegradable (>90%) within 120 days. Instead, 17:3 films, although of biological origin, did not reach complete biodegradability, reaching a maximum of 77 and 52%, for films with and without MAP enrichment, respectively (Figure 3). Previous mesocosm experiments and open-field trials on 1:1 MAP-enriched films [33] have shown no critical increases in soil electrical conductivity or pH, nor adverse effects on plant growth under realistic cultivation conditions, supporting the agronomic compatibility of the proposed formulations. In addition, field observations reported in [33] suggest that, despite their hydrophilic nature, the films do not dissolve immediately after soil application; instead, they maintain structural integrity during the initial use phase and undergo a progressive loss of cohesion after placement, rather than rapid dissolution.

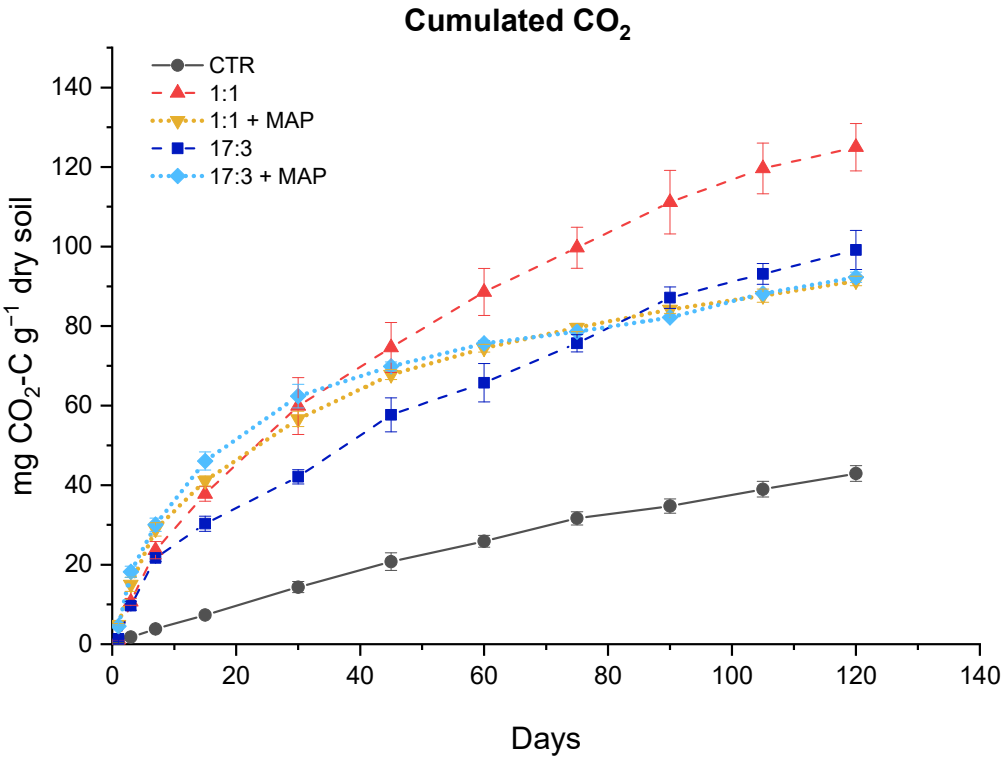


Figure 2. Cumulative CO_2-C production (mg CO_2-C g^{-1} dry soil) over time (days) for soil samples added with different bio-based films (1:1, 1:1 + MAP, 17:3, and 17:3 + MAP) and for the control (CTR). Values represent mean (n = 4) ± standard deviation (SD).

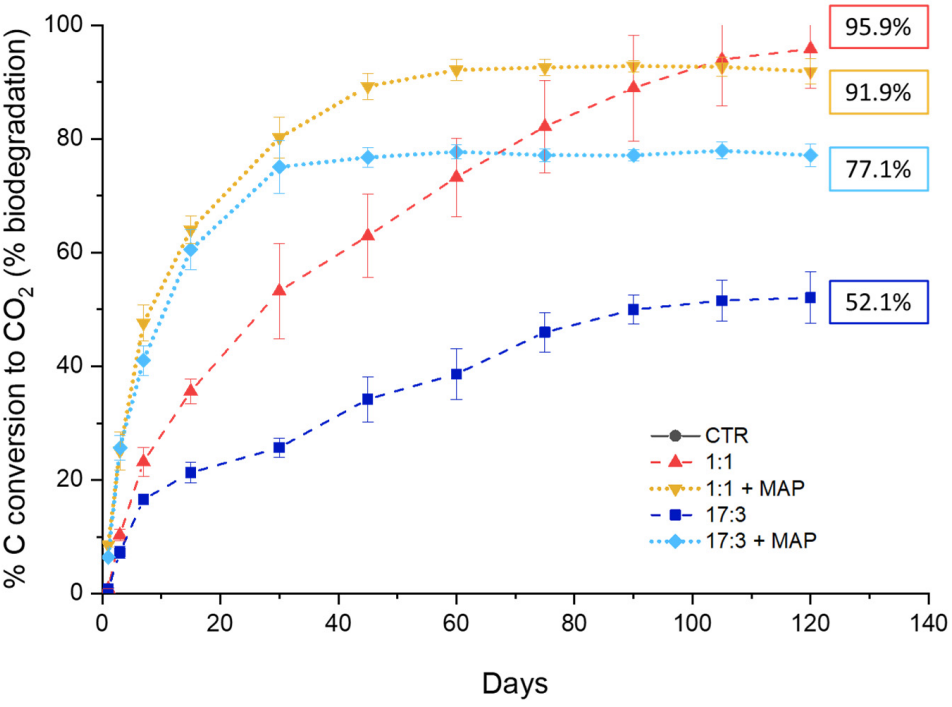


Figure 3. Biodegradation (%) of the different films in soil over time (days). Values represent mean (n = 4) ± standard deviation (SD).

Further investigations, including mass loss analysis, degradation product characterization, and the evaluation of different MAP contents, are warranted to provide a more comprehensive understanding of the biodegradation mechanisms.

3.3. Films' Analysis with Pyrolysis–Gas Chromatography

Py-GC-MS of the 1:1 mulching films, with and without MAP enrichment, yielded qualitatively similar pyrograms comprising 31 annotated products (Table 2) with their putative precursors. Within the resolution of Py-GC-MS, CMC and SA cannot be discriminated because their carbohydrate backbones decompose to largely overlapping product suites. On the contrary, chitosan subjected to pyrolysis produces, in addition to the compounds derived from polysaccharides, also typical nitrogen-containing heterocyclic markers, such as pyrrole, pyridine, and pyrazine derivatives. In addition, characteristic compounds (acetic acid and methylurea) produced, under pyrolysis conditions, from the N-acetyl group of chitosan are well represented [27,34]. The results suggest that in their active phase of degradation, mulches can differentially contribute to soil organic composition, potentially influencing organic carbon dynamics and microbial activity. In contrast, the chitosan component generated nitrogen-containing heterocycles (pyrroles, pyridines, and pyrazines) together with urea-type derivatives (e.g., methylurea) and additional acetic acid arising from N-acetyl cleavage [27,34], providing a distinct nitrogenous fingerprint. In films without MAP, the relative abundances of furan/aldehyde markers and of pyrroles/pyridines indicate a balanced contribution of the carboxymethyl cellulose- and chitosan-rich domains.

Table 2. Retention times (RT), qualitative abundances very low (+), medium (++), high (+++), very high (++++), and assignments to chitosan (CS), carboxymethyl cellulose (CMC), and sodium alginate (SA) of pyrolysis products of bio-based films (1:1 and 1:1 + MAP).

RT (min)	Compound	MW, Base Peak	Origin	Relative Abundance	
				1:1	1:1 + MAP
1.48	2-Propenal	56, 56	CS, CMC	++	++
1.65	1,3-Cyclopentadiene	66, 66	CS, CMC	++	–
1.81	2,3-Butanedione	86, 86	SA, CMC	++	–
1.85	2-Methyl furan	82, 82	SA, CMC	++	+
1.86	Butanal	72, 72	SA, CMC	+	–
2.16	1,3-Cyclohexadiene	80, 79	CMC	+	–
2.25	Acetic acid	60, 60	SA, CMC, CS	+	–
2.59	Methylurea	74, 74	CS	+	+
2.63	3,3-Dimethyl-2-butanone	100, 57	SA, CMC	++	–
3.09	Pyrazine	80, 80	CS	+	–
3.23	1-Methyl pyrrole	81, 80	CS	+	–
3.33	Pyridine	79, 79	CS	+	+++
3.44	Pyrrole	67, 67	CS	+	–
3.71	1-Hydroxy-2-butanone	88, 57	CMC	+	–
3.97	3-Butenal-2-one	84, 84	SA, CMC	+	–
4.34	3-Furaldehyde	96, 95	CMC	+	–
4.37	2-Methyl pyridine	93, 93	CS	–	++++
4.52	Methylpyrazine	94, 94	CS	+	–
4.72	(Furfural) + (3-methyl furan)	(96, 95) + (82, 82)	SA, CS, CMC	++	+
4.83	2-Methyl cyclopentanone	98, 55	SA, CMC	+	–
4.85	3-Methyl, 1H-Pyrrole	81, 80	CS	+	+
5.17	4-Methyl pyridine	93, 93	CS	–	++++
6.04	2-Methyl-2-cyclopenten-1-one	96, 67	SA, CMC	+++	+

Table 2. *Cont.*

RT (min)	Compound	MW, Base Peak	Origin	Relative Abundance	
				1:1	1:1 + MAP
6.21	Ethyl pyrazine	108, 107	CS	+	+
6.63	1-Isopropylcyclopentene	110, 67	SA, CMC	+	–
7.14	3-Methyl-2-cyclopenten-1-one	96, 96	SA, CMC	+++	–
8.16	Acetylpyrazine	122, 80	CS	+	–
8.49	2-Hydroxy-1-methyl-1-cyclopenten-3-one	112, 112	SA, CMC	++	–
8.52	2,3-Dimethyl-2-cyclopenten-1-one	110, 67	SA, CMC	++	–
8.91	2-Hydroxy-3-ethyl-2-cyclopenten-1-one	126, 126	SA, CMC	++++	–
13.09	Acetamidomethylfuran	139, 97	CS	+	–

Among nitrogen-containing heterocyclic compounds, pyridine derivatives are significantly more present in the pyrolysis products of the MAP-enriched film, while pyrrole and pyrazine derivatives remain at a more or less constant level. Probably, the presence of ammonium favors the rearrangement to an energetically stable six-membered and aromatic structure such as pyridine. This chemical differentiation allows a specific fingerprint to be attributed to each treatment, confirming that MAP acts as a discriminating factor in the chemical composition of the soil after the application of the mulch. This behavior must be considered in the design of functionalized biodegradable mulches, especially in agricultural applications where the interaction with the soil and the microbiome can be influenced by the release of these compounds.

Pyrolysis products of Mater-Bi are shown in Table 3. Among the fifteen peaks annotated, those corresponding to the lactone 1,6-dioxacyclododecane-7,12-dione (16.56 min), cyclopentanone (4.27 min, the most abundant), and esters of adipic (16.13 and 18.62 min), phthalic (19.67 min), and terephthalic (21.92 min) acids are correlated to the presence of poly(butylene adipate-co-butylene terephthalate), PBAT [20,35]. In addition, pyrolysis products originated from starch are present: pyruvic aldehyde (1.67 min) and levoglucosane (15.59 min) [20]. The Mater-Bi analyzed, therefore, consists essentially of two components, starch and PBAT, the latter being a biodegradable polymer but synthetically produced from precursors of fossil origin.

Table 3. Retention times (RT), qualitative abundances very low (+), medium (++), high (+++), and molecular weights (MW) of pyrolysis products of Mater-Bi.

RT (min)	Compound	MW, Base Peak	Relative Abundance
1.56	1,3-butadiene	54, 54	++
1.67	Pyruvic aldheyde	72, 43	+
2.32	Tetrahydrofuran	72, 42	++
4.27	Cyclopentanone	84, 55	+++
9.37	Pentanoic acid, 3-butenyl ester	156, 85	+
11.06	Benzoic acid	122, 105	+
13.83	Benzoic acid, 3-butenyl ester	176, 105	++
14.29	Biphenyl	154, 154	+
15.59	Levoglucosane	162, 60	++
16.13	Adipic acid, 3-butenyl ester	129, 129	++
16.55	1,6-Dioxacyclododecane-7,12-dione	200, 55	+
18.62	Adipic acid, di(3-butenyl) ester	254, 55	++
19.67	Phthalic acid, monobut-3-enyl ester	220, 149	++
21.08	Hexadecanoic acid	256, 73	+
21.92	Terephthalic acid, di(3-butenyl) ester	274, 203	++

4. Conclusions

This study introduces a new class of fully bio-based mulch films composed exclusively of natural polysaccharides (chitosan, carboxymethyl cellulose, and sodium alginate), with or without monoammonium phosphate (MAP) enrichment. The 1:1 formulation, either enriched or not with MAP, achieved biodegradation levels exceeding 90% within 120 days, matching international criteria for soil biodegradability. A key strength of the developed films lies in their entirely bio-based nature, which distinguishes them from widely used commercial biodegradable mulches, such as Mater-Bi, that still include polymeric fractions derived from fossil resources. This characteristic ensures not only effective biodegradation in soil but also a reduced dependence on non-renewable feedstocks, thereby enhancing the overall environmental sustainability of the material. Beyond these shared advantages of the 1:1 films, MAP enrichment provides an additional, distinctive function: the 1:1 + MAP formulation acts as a nutrient-releasing mulch, supplying N and P during soil exposure, as supported by isotopic tracing and Py-GC-MS evidence of MAP incorporation and related structural and chemical modifications. From a practical standpoint, the 1:1 formulation emerges as the most promising candidate for further development and field testing, whereas the 17:3 formulation, despite its fully bio-based origin, showed limited biodegradability under the tested conditions. Overall, these findings demonstrate the potential of fully bio-based, multifunctional mulch films as soil-friendly alternatives to current commercial products, contributing to more sustainable and circular agricultural practices.

Supplementary Materials: The following supporting information can be downloaded at: https://www.mdpi.com/article/10.3390/horticulturae12020253/s1, Figure S1: Conceptual model of nitrogen heterogeneity at high MAP loadings. Schematic representation of a non-homogeneous nitrogen distribution within the polymer matrix, where MAP-rich regions (NH_4^+-derived nitrogen) coexist with polymer-rich (chitosan-rich) domains. Such spatial segregation may lead to non-ideal isotopic mixing, causing bulk $\delta^{15}N$ values to deviate from a linear relationship with MAP content at high salt loadings.

Author Contributions: Conceptualization, S.P., D.F.C.M. and V.A.L.; data curation, S.P. and V.V.; funding acquisition, V.A.L.; investigation, S.P., V.C.C., V.V. and V.A.L.; methodology, S.P. and V.V.; resources, V.A.L.; supervision, V.A.L.; writing—original draft, S.P., V.C.C., V.V. and V.A.L.; writing—review and editing, S.P., L.B., D.F.C.M., V.C.C., S.R.S., E.A., V.V. and V.A.L. All authors have read and agreed to the published version of the manuscript.

Funding: This research was funded by the Italian Ministry of Education, University, and Research (MUR) through the PRIN 2020 project PRJ-0761.

Data Availability Statement: Data is contained within the article or Supplementary Material.

Conflicts of Interest: The authors declare no conflicts of interest.

Abbreviations

The following abbreviations are used in this manuscript:

Abbreviation	Definition
CMC	Carboxymethyl cellulose
CS	Chitosan
SA	Sodium alginate
MAP	Monoammonium phosphate
EA-IRMS	Elemental analyzer–isotope ratio mass spectrometry
Py-GC-MS	Pyrolysis–gas chromatography–mass spectrometry
PE	Polyethylene

PBAT	Poly(butylene adipate-co-butylene terephthalate)
PCL	Poly(ε-caprolactone)
PET	Polyethylene terephthalate
PEF	Polyethylene furanoate
GHG	Greenhouse gases
TOC	Total organic carbon
TN	Total nitrogen
CEC	Cation exchange capacity
CTR	Control (soil without film addition)
WHC	Water holding capacity
RT	Retention time
Mw	Molecular weight
XRD	X-ray diffraction

References

1. Plastics Europe. *Plastics—The Facts 2022*; Plastics Europe: Brussels, Belgium, 2022. Available online: https://plasticseurope.org/knowledge-hub/plastics-the-facts-2022/ (accessed on 1 March 2025).
2. Menossi, M.; Cisneros, M.; Alvarez, V.A.; Casalongué, C. Current and emerging biodegradable mulch films based on polysaccharide bio-composites: A review. *Agron. Sustain. Dev.* **2021**, *41*, 53. [CrossRef]
3. Pathak, G.; Nichter, M.; Hardon, A.; Moyer, E.; Latkar, A.; Simbaya, J.; Love, J. Plastic pollution and the open burning of plastic wastes. *Glob. Environ. Change* **2023**, *80*, 102648. [CrossRef]
4. Sa'adu, I.; Farsang, A. Plastic contamination in agricultural soils: A review. *Environ. Sci. Eur.* **2023**, *35*, 13. [CrossRef]
5. D'Avino, L.; Rizzuto, G.; Guerrini, S.; Sciaccaluga, M.; Pagnotta, E.; Lazzeri, L. Environmental implications of crude glycerin used in special products for the metalworking industry and in biodegradable mulching films. *Ind. Crops Prod.* **2015**, *75*, 29–35. [CrossRef]
6. Razza, F.; Guerrini, S.; Impallari, F.M. How sustainable biodegradable and renewable mulch films are? A quantitative approach in the light of sustainable development goals. In *Proceedings of the XXI International Congress on Plastics in Agriculture: Agriculture, Plastics and Environment*; Acta Horticulturae: Leuven, Belgium, 2019; Volume 1252, pp. 77–84. [CrossRef]
7. Li, X.; Zheng, G.; Li, Z.; Fu, P. Formulation, performance and environmental/agricultural benefit analysis of biomass-based biodegradable mulch films: A review. *Eur. Polym. J.* **2024**, *203*, 112663. [CrossRef]
8. Campanale, C.; Galafassi, S.; Di Pippo, F.; Pojar, I.; Massarelli, C.; Uricchio, V.F. A critical review of biodegradable plastic mulch films in agriculture: Definitions, scientific background and potential impacts. *TrAC Trends Anal. Chem.* **2024**, *170*, 117391. [CrossRef]
9. Yang, N.; Ying, L.; Li, K.; Chen, F.; Zhao, F.; Sun, Z.; Liu, J. Biodegradable mulching films based on polycaprolactone and its porous structure construction. *Polymers* **2022**, *14*, 5340. [CrossRef]
10. Hatti-Kaul, R.; Nilsson, L.J.; Zhang, B.; Rehnberg, N.; Lundmark, S. Designing biobased recyclable polymers for plastics. *Trends Biotechnol.* **2020**, *38*, 50–67. [CrossRef]
11. Eerhart, A.J.J.E.; Faaij, A.P.C.; Patel, M.K. Replacing fossil based PET with biobased PEF: Process analysis, energy and GHG balance. *Energy Environ. Sci.* **2012**, *5*, 6407–6422. [CrossRef]
12. Nova Institute. *Bio-Based Building Blocks and Polymers—Global Capacities, Production and Trends 2019–2024*; Nova Institute: Hürth, Germany, 2019. Available online: http://nova-institute.eu/press/?id=164 (accessed on 1 March 2025).
13. Pinaeva, L.G.; Noskov, A.S. Biodegradable biopolymers: Real impact to environment pollution. *Sci. Total Environ.* **2024**, *947*, 174445. [CrossRef]
14. *ISO 17556*; Plastics—Determination of the Ultimate Aerobic Biodegradability of Plastic Materials in Soil by Measuring the Oxygen Demand in a Respirometer or the Amount of Carbon Dioxide Evolved. International Organization for Standardization: Geneva, Switzerland, 2019.
15. *EN 17033*; Plastics-Biodegradable Mulch Films for Use in Agriculture and Horticulture-Requirements and Test Methods. European Standard; European Committee for Standardization: Brussels, Belgium, 2018.
16. Chinaglia, S.; Tosin, M.; Degli-Innocenti, F. Biodegradation rate of biodegradable plastics at molecular level. *Polym. Degrad. Stab.* **2018**, *147*, 237–244. [CrossRef]
17. Sander, M. Biodegradation of polymeric mulch films in agricultural soils: Concepts, knowledge gaps, and future research directions. *Environ. Sci. Technol.* **2019**, *53*, 2304–2315. [CrossRef] [PubMed]

18. Zumstein, M.T.; Schintlmeister, A.; Nelson, T.F.; Baumgartner, R.; Woebken, D.; Wagner, M.; Kohler, H.-P.E.; McNeill, K.; Sander, M. Biodegradation of synthetic polymers in soils: Tracking carbon into CO_2 and microbial biomass. *Sci. Adv.* **2018**, *4*, eaas9024. [CrossRef] [PubMed]
19. Berto, D.; Rampazzo, F.; Gion, C.; Noventa, S.; Ronchi, F.; Traldi, U.; Giorgi, G.; Cicero, A.M.; Giovanardi, O. Preliminary study to characterize plastic polymers using elemental analyser/isotope ratio mass spectrometry (EA/IRMS). *Chemosphere* **2017**, *176*, 47–56. [CrossRef]
20. De Falco, F.; Nacci, T.; Durndell, L.; Thompson, R.C.; Degano, I.; Modugno, F. A thermoanalytical insight into the composition of biodegradable polymers and commercial products by EGA-MS and Py-GC-MS. *J. Anal. Appl. Pyrolysis* **2023**, *171*, 105937. [CrossRef]
21. Okoffo, E.D.; Rauert, C.; Thomas, K.V. Mass quantification of microplastic at wastewater treatment plants by pyrolysis-gas chromatography–mass spectrometry. *Sci. Total Environ.* **2023**, *856*, 159251. [CrossRef]
22. Ciaramitaro, V.; Piacenza, E.; Paliaga, S.; Cavallaro, G.; Badalucco, L.; Laudicina, V.A.; Chillura Martino, D.F. Exploring the feasibility of polysaccharide-based mulch films with controlled ammonium and phosphate ions release for sustainable agriculture. *Polymers* **2024**, *16*, 2298. [CrossRef]
23. Paliaga, S.; Badalucco, L.; Ciaramitaro, V.C.; Chillura Martino, D.F.; Gelsomino, A.; Kandeler, E.; Marhan, S.; Laudicina, V.A. Fertilizer enriched bio-based mulch films increase nitrogen and phosphorus availability and stimulate soil microbial biomass and activity. *Appl. Soil Ecol.* **2025**, *211*, 106159. [CrossRef]
24. Jones, B.J., Jr.; Case, V.W. Sampling, handling, and analyzing plant tissue samples. In *Soil Testing and Plant Analysis*, 3rd ed.; Westerman, R.L., Ed.; Soil Science Society of America: Madison, WI, USA, 1990; Volume 3, pp. 389–427.
25. Liu, X.; Wang, D.; Bazhabaike, M.; Zhou, M.; Yin, T. Biodegradable Film Mulching Increases Soil Respiration: A Two-Year Field Comparison with Polyethylene Film Mulching in a Semi-Arid Region of Northern China. *Agronomy* **2025**, *15*, 2631. [CrossRef]
26. Kaczmarska, K.; Żymankowska-Kumon, S.; Byczyński, Ł.; Grabowska, B.; Bobrowski, A.; Cukrowicz, S. Thermoanalytical studies (TG–DTG–DSC, Py–GC/MS) of sodium carboxymethyl starch with different degrees of substitution. *J. Therm. Anal. Calorim.* **2019**, *138*, 4417–4425. [CrossRef]
27. Sato, H.; Mizutani, S.; Tsuge, S. Determination of the degree of acetylation of chitin/chitosan by pyrolysis-gas chromatography in the presence of oxalic acid. *Anal. Chem.* **1998**, *70*, 7–12. [CrossRef]
28. Bateman, A.S.; Kelly, S.D. Fertilizer Nitrogen Isotope Signatures. *Isot. Environ. Health Stud.* **2007**, *43*, 237–247. [CrossRef] [PubMed]
29. Perini, M.; Nardin, T.; Venturelli, M.; Pianezze, S.; Larcher, R. Stable isotope ratio analysis as a fast and simple method for identifying the origin of chitosan. *Food Hydrocoll.* **2020**, *101*, 105516. [CrossRef]
30. Polman, E.M.; Gruter, G.J.M.; Parsons, J.R.; Tietema, A. Comparison of the aerobic biodegradation of biopolymers and the corresponding bioplastics: A review. *Sci. Total Environ.* **2021**, *753*, 141953. [CrossRef] [PubMed]
31. Reay, M.K.; Graf, M.; Greenfield, L.M.; Bargiela, R.; Onyije, C.; Lloyd, C.E.; Jones, D.L. Microbial degradation of bioplastic (PHBV) is limited by nutrient availability at high microplastic loadings. *Environ. Sci. Adv.* **2025**, *4*, 133–146. [CrossRef]
32. Rossetti, I.; Conte, F.; Ramis, G. Kinetic modelling of biodegradability data of commercial polymers obtained under aerobic composting conditions. *Eng* **2021**, *2*, 54–68. [CrossRef]
33. Pittarello, M.; Rodinò, M.T.; Sidari, R.; Panuccio, M.R.; Cozzi, F.; Branca, V.; Petrovičová, B.; Gelsomino, A. Employment of Biodegradable, Short-Life Mulching Film on High-Density Cropping Lettuce in a Mediterranean Environment: Potentials and Prospects. *Agriculture* **2025**, *15*, 1219. [CrossRef]
34. Furuhashi, T.; Beran, A.; Blazso, M.; Czegeny, Z.; Schwarzinger, C.; Steiner, G. Pyrolysis GC/MS and IR spectroscopy in chitin analysis of molluscan shells. *Biosci. Biotechnol. Biochem.* **2009**, *73*, 93–103. [CrossRef]
35. Rizzarelli, P.; Rapisarda, M.; Perna, S.; Mirabella, E.F.; La Carta, S.; Puglisi, C.; Valenti, G. Determination of polyethylene in biodegradable polymer blends and in compostable carrier bags by Py-GC/MS and TGA. *J. Anal. Appl. Pyrolysis* **2016**, *117*, 72–81. [CrossRef]

Disclaimer/Publisher's Note: The statements, opinions and data contained in all publications are solely those of the individual author(s) and contributor(s) and not of MDPI and/or the editor(s). MDPI and/or the editor(s) disclaim responsibility for any injury to people or property resulting from any ideas, methods, instructions or products referred to in the content.